11-12-2015

MASH TL-4 Design and Evaluation of A Restorable Energy-Absorbing Concrete Barrier

Jennifer D. Schmidt
University of Nebraska-Lincoln, jennifer.rasmussen@unl.edu

Scott K. Rosenbaugh
University of Nebraska - Lincoln, srosenbaugh2@unl.edu

Robert W. Bielenberg
University of Nebraska - Lincoln, rbielenberg2@unl.edu

Ronald K. Faller
University of Nebraska - Lincoln, rfaller1@unl.edu

John D. Reid
University of Nebraska - Lincoln, jreid@unl.edu

See next page for additional authors

Paper No. 16-0650

Transportation Research Record: Journal of the Transportation Research Board, No. 2588, Best Paper Award - TRB AFB20 Committee on Roadside Safety Design, Transportation Research Board, Washington D.C., DOI 10.3141/2588-11, pages 98-109, January 2016

MASH TL-4 Design and Evaluation of A Restorable Energy-Absorbing Concrete Barrier

by

Jennifer D. Schmidt, Ph.D., P.E.
Midwest Roadside Safety Facility
University of Nebraska-Lincoln
130 Whittier Building
2200 Vine Street
Lincoln, Nebraska 68583-0853
Phone: (402) 472-0870
Fax: (402) 472-2022
Email: jennifer.schmidt@unl.edu
(Corresponding Author)

Scott K. Rosenbaugh, M.S.C.E.
Midwest Roadside Safety Facility
University of Nebraska-Lincoln
130 Whittier Building
2200 Vine Street
Lincoln, Nebraska 68583-0853
Phone: (402) 472-9324
Fax: (402) 472-2022
Email: srosenbaugh2@unl.edu

Robert W. Bielenberg, M.S.M.E.
Midwest Roadside Safety Facility
University of Nebraska-Lincoln
130 Whittier Building
2200 Vine Street
Lincoln, Nebraska 68583-0853
Phone: (402) 472-9064
Fax: (402) 472-2022
Email: rbielenberg2@unl.edu

Ronald K. Faller, Ph.D., P.E.
Midwest Roadside Safety Facility
University of Nebraska-Lincoln
130 Whittier Building
2200 Vine Street
Lincoln, Nebraska 68583-0853
Phone: (402) 472-6864
Fax: (402) 472-2022
Email: rfaller1@unl.edu

John D. Reid, Ph.D.
Mechanical & Materials Engineering
Midwest Roadside Safety Facility
University of Nebraska-Lincoln
W342 NH (0526)
Lincoln, Nebraska 68588
Phone: (402) 472-3084
Fax: (402) 472-1465
Email: jreid@unl.edu

Tyler L. Schmidt, B.S.C.E.
Midwest Roadside Safety Facility
University of Nebraska-Lincoln
130 Whittier Building
2200 Vine Street
Lincoln, Nebraska 68583-0853
Phone: (402) 472-9043
Fax: (402) 472-2022
Email: t.schmidt@huskers.unl.edu

Submitted to

Transportation Research Board
95th Annual Meeting
January 10-14, 2016
Washington, D.C.

November 12, 2015

Length of Paper: 4,819 (text) + 250x8 (8 figures and 0 tables) + 500 (references) = 7,319 words

ABSTRACT

A new, high-containment longitudinal barrier was designed to reduce the accelerations imparted to passenger vehicles during impacts and to be restorable and reusable. Elastomer support posts were designed to translate laterally and absorb energy when impacted and restore to their initial position after impact events. A hybrid concrete beam and steel tube combination rail was optimized to minimize weight, provide sufficient structural capacity, maintain a height to contain and redirect single-unit trucks, and to prevent passenger vehicles from snagging on the posts. Three full-scale vehicle crash tests were conducted according to *Manual for Assessing Safety Hardware* (MASH) Test Level (TL-4) safety performance requirements on a 240-ft long barrier with nominal height of 38⅝ in. In test SFH-1, a 5,021-lb pickup truck was redirected with minimal damage to the barrier. The peak lateral acceleration was reduced 47 percent as compared to similar impacts on rigid barriers. In test SFH-2, a 2,406-lb small car was redirected by the barrier, and the peak lateral acceleration was reduced 21 percent as compared to similar impacts on rigid barriers. In test SFH-3, a 21,746-lb single-unit truck was successfully contained and redirected, resulting in only minor damage to the concrete rail. Therefore, the barrier met all MASH TL-4 safety performance criteria. Recommendations about the performance, future design refinements, and installation requirements of the barrier were provided.

Keywords: Highway Safety, Crash Test, Compliance Test, MASH, Test Level 4, Energy Absorbing Barrier, Low Maintenance, Rubber Posts, Elastomers

INTRODUCTION

Rigid concrete barriers have proven successful at containing and redirecting large trucks and passenger vehicles during impact events. Even though rigid concrete barrier have acceptable occupant risk measures during full-scale crash testing, passenger vehicle impacts into concrete barriers can still result in severe and fatal injuries to the occupants due to the non-forgiving nature of the barrier. Certain barrier shapes, such as the New Jersey barrier, can also increase vehicle climb and the potential for rollover. Therefore, a forgiving, restorable, energy-absorbing longitudinal barrier concept was developed by Schmidt, et al. (*1-4*) that would reduce the lateral acceleration imparted to occupants during passenger vehicle impacts, while still redirecting large trucks.

There were several design criteria for the barrier. First, the barrier was to satisfy the AASHTO *Manual for Assessing Safety Hardware* (MASH) Test Level 4 (TL-4) performance evaluation criteria (*5*). Also, a 30 percent decrease in lateral acceleration for passenger vehicles was desired with impacts into the new barrier, as compared to similar impacts with rigid concrete barriers. Furthermore, the barrier width needed to be less than or equal to 36 in. to accommodate current urban median footprint widths. The system was to be restorable and reusable with no damage occurring during passenger vehicle impacts. A minimal amount of damage was permissible with single-unit truck impact events. Therefore, the objective was to design and evaluate a new restorable and reusable energy-absorbing barrier according to the MASH TL-4 requirements and also meet the established design criteria.

LITERATURE REVIEW

Numerous crash cushions, guardrail end terminals, roadside barriers, and other applications utilize energy-absorbing mechanisms to minimize forces during dynamic impacts. Crash cushions utilize mechanisms such as:

1. transfer of momentum into an expendable mass;
2. crushing of energy-dissipating cartridges;
3. compression of shock-arresting cylinders;
4. elastic deformation of restorable HDPE plates; and
5. compression of pressurized membrane shock absorbers.

Additionally, many energy-absorbing guardrail end terminals utilize mechanisms such as kinking, flattening, or cutting of steel rail segments. These energy absorbing mechanisms are summarized in the report by Schmidt, et al (*1-2*).

The Steel And Foam Energy Reduction (SAFER) barrier was successfully developed for use in high-speed racetrack applications for the purpose of reducing the severity of race car crashes into rigid concrete containment walls (*6-12*). The barrier consists of a vertical-face, steel impact panel offset from a rigid concrete wall with discrete, energy-absorbing foam cartridges that dissipate the impacting vehicle's kinetic energy. Prior to the installation of the SAFER barrier at all National Association for Stock Car Auto Racing (NASCAR) and INDYCAR high-speed oval racetracks, an average of 1½ deaths occurred per year during impacts with the outer rigid containment barriers. No fatal crashes involving outer wall impacts have been reported since the installation of the SAFER barrier. While vehicle decelerations were reduced by approximately 30 percent with the SAFER barrier during full-scale crash testing, the foam cartridges often need to be replaced after high-energy impact events.

Dating back to the 1970s, innovative longitudinal barriers and bridge rails were developed, incorporating collapsible steel or rubber cylinders to mitigate accelerations and minimize damaged system parts when impacted. Unfortunately, many of these systems are not widely utilized. An energy-absorbing bridge rail was developed at the Texas A&M Transportation Institute in 2010 (*13*). The bridge rail contained two steel tube rails with a laterally-loaded collapsible steel pipe attached to a concrete parapet. Two full-scale crash tests were conducted according to MASH, but at higher speeds around 85 mph. The small car test was successful, and the barrier dynamically deflected 7.5 in. The pickup truck redirected and exited the system, and then subsequently rolled. While many crash cushions and past bridge rails have utilized specific energy-absorbing materials, they are not widely used in longitudinal barriers today. Therefore, several energy-absorbing materials and mechanisms were further explored for their use in this energy-absorbing barrier.

DESIGN METHODOLOGY AND DETAILS

Several barrier concepts were investigated during the design process, including a wide variety of energy-absorbing materials and mechanisms. Various materials, including elastomers (rubber), HDPE, foam, air baffles, sorbothane, and coil springs, were explored. Elastomers were selected based on their restorability, resistance to environmental degradation, ability to be molded into any shape, and successful performance in other roadside safety applications.

The impact face of the barrier system needed to be constructed of a durable material to prevent damage during impact events. Steel rails were considered, but thought to be too expensive as multiple rails would be necessary on each side of a median barrier configuration. Subsequently, reinforced concrete was selected, as concrete barriers can redirect heavy trucks while sustaining minimal damage. To incorporate energy absorbers into the barrier, elastomer posts were utilized to support the concrete rail. The elastomer posts would allow the barrier to translate laterally, extend the time of the impact event, reduce the forces imparted to the vehicle, and apply a restoration force to the deflected barrier to bring it back to its original position. Thus, the combination of a concrete rail and elastomer posts created a durable, low maintenance system that deforms and absorbs energy when impacted and then restores itself afterward. Photographs of the design selected for further evaluation via computer simulation and full-scale crash testing is shown in FIGURE 1 (*4,14*).

The development of a new elastomer post would have been time consuming and costly as new molds would have been required for fabrication. Therefore, several existing pre-fabricated elastomer parts were investigated as potential posts for the barrier system. Of these pre-existing parts, shear fenders, typically used for marine, ship docking applications, showed the most promise. Shear fenders are elastomer blocks that deform in shear (i.e., one side of the shear fender translates while the other remains stationary) and provide a lateral resistance force until it returns to its original position. Shear fenders are manufactured in multiple sizes, but the shortest available shear fender was selected for use in order to minimize the risk of a small car underriding the concrete beam and impacting the post. The selected shear fender measured 11⅝ in. tall x 10 in. long x 15¾ in. wide and utilized four ¾-in. diameter bolts to attach the shear fender to the concrete beam.

The concrete rail needed to be at least 21½ in. wide for the shear fender attachment bolts to fit inside the internal steel reinforcement of the beam. Additionally, a minimum 36-in. barrier height was deemed necessary to prevent the MASH single-unit truck from rolling over the barrier. However, a concrete beam satisfying these geometrical requirements would have a large

mass, which would hinder translation during small vehicle impacts. Thus, three different methods were utilized to minimize the weight of the rail segments. First, lightweight concrete with a density of 110 pcf and a minimum 28-day compressive strength of 5,000 psi was utilized for the beam. Second, 6⅝-in. diameter vertical holes were placed along the centerline of the beam. Finally, the top 6 in. of the beam was removed and replaced with a 8-in. x 4-in. x ¼-in. steel tube mounted to the top of the concrete rail using 4-in. tall steel support posts. The result was a hybrid concrete beam and steel tube rail that was optimized to minimize weight, provide sufficient structural capacity, and provide an overall barrier height of 38⅝ in.

The concrete beams were 18½ in. tall x 21½ in. wide and were fabricated with a length of 19 ft – 11½ in. The upper steel tube segments were cut to the same length and were spliced at the mid-point of the concrete beams. The steel tube support posts were placed directly above each elastomer post, and four ¾-in. diameter threaded rods attached the steel tube, the concrete beam, and elastomer post together.

To achieve the desired acceleration reductions, the impact force needed to be distributed to multiple elastomer posts. Therefore, the rail splices needed to provide continuity (shear and moment transfer) between adjacent rail segments and allow the impact force to be distributed to the greatest number of posts. Additionally, a joint was desired that could account for a variable gap between adjacent segments due to fabrication and construction tolerances. An adjustable continuity joint was developed and consisted of steel angles placed on the front and back side at the ends of the beams. The vertical edges on the ends of each concrete segment were angled at 45 degrees, which created a triangular pocket on the front and back sides of the rail at each splice location. The steel angles were then placed within the pockets and bolted through to a hollow cavities in the center of the concrete beams. The angles were designed to provide tension, compression, and shear across both the front and back face of each concrete joint. Thus, moment continuity was achieved. Additionally, the angles allowed for +/- ¼-in. of tolerance in the ½-in. nominal spacing between adjacent segments. Development and further details of the joint can be found in Schmidt, et al. (*4*).

The continuity of the system and the distribution of impact forces to posts were evaluated using analytical calculations, dynamic component tests, and computer simulation. The energy absorbing characteristics of the posts were evaluated with dynamic component tests (*3-4*). The results from these tests were utilized in analytical calculations as well as computer simulation to predict barrier displacement and vehicle accelerations associated with various post spacings. Ultimately, MASH TL-3 impacts with a 5,000-lb pickup truck into the system with a post spacing of 60 in. caused 8 in. to 10 in. of barrier displacement and reduced lateral accelerations by approximately 30 percent (*1-4*), which was the original design criteria. Therefore, a 60-in. spacing, or ¼ the length of a concrete beam segment, was selected for the elastomer posts.

Although initial static component testing demonstrated that the elastomer posts could support the beam weight, variations in real world installations led to the addition of steel support skids to increase the system stability (*3-4*). The skids supported the majority of the combination rail's weight. The skids also restricted the rotation of the barrier during computer simulation impact events. This restriction allowed the shear fenders to function more efficiently and helped the barrier restore (*4*).

The final system configuration that was recommended for full-scale testing was a median barrier with a total length of 239 ft - 11½ in., which consisted of twelve precast reinforced-concrete beams and upper tube assemblies. Each beam was supported by four elastomer posts and two steel skids. The posts were spaced at 60 in. on-center, while the skids were spaced at 120 in. on-center. Each post was anchored to the tarmac with four ¾-in. diameter threaded rod

anchors embedded 8 in. and epoxy. Details of the barrier system are shown in FIGURE 2. Full system design details are found in Schmidt, et al. (*14*).

FIGURE 1 View of initial concept with elastomer posts and metal skids (*4,14*).

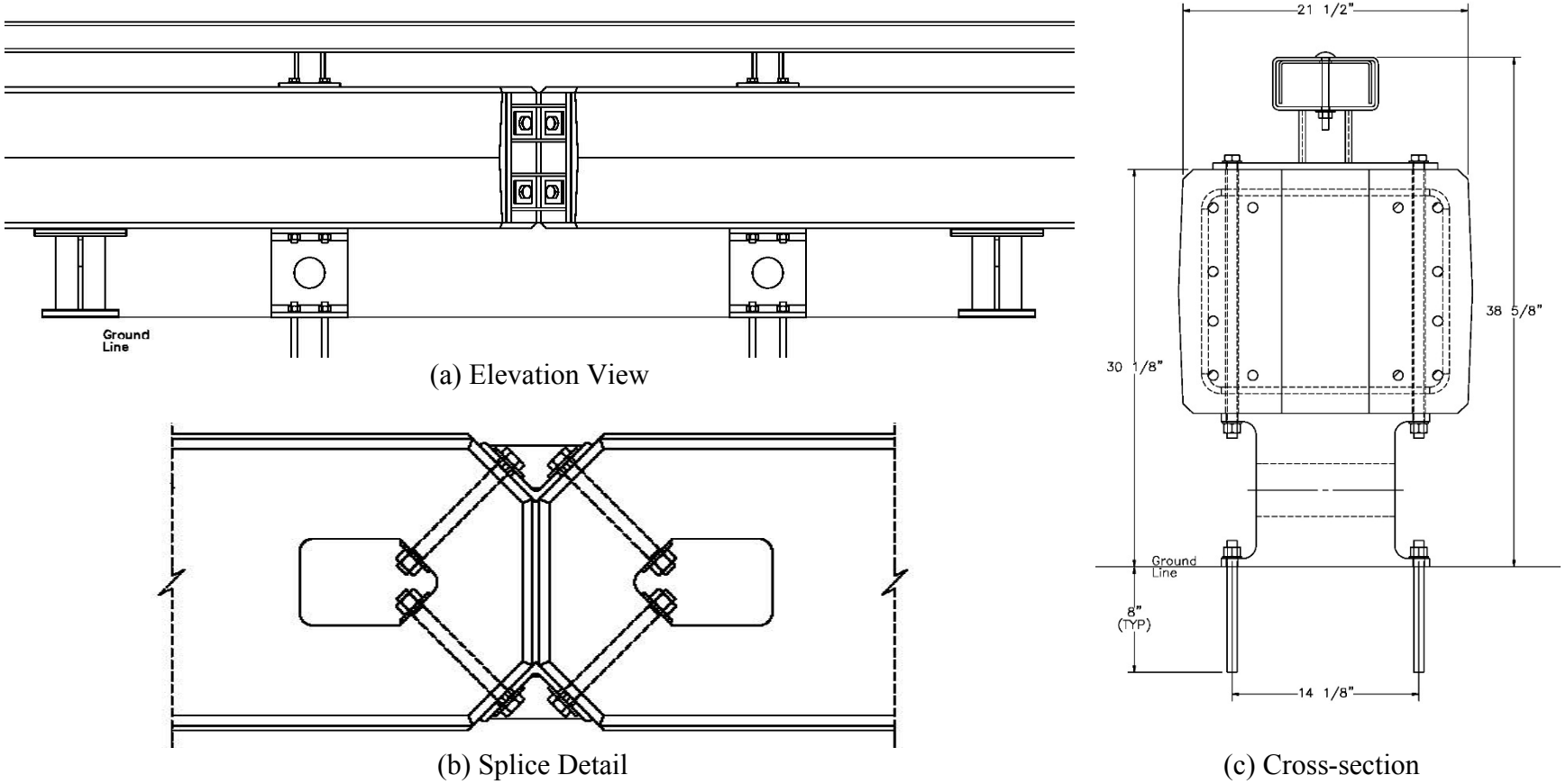

(a) Elevation View

(b) Splice Detail

(c) Cross-section

FIGURE 2 System details of the barrier, (a) elevation view, (b) splice detail, and (c) cross-section (*14*).

TEST REQUIREMENTS AND EVALUATION CRITERIA

Longitudinal barriers, such as concrete barriers, must satisfy impact safety standards in order to be eligible for reimbursement by the Federal Highway Administration for use on the National Highway System. For new hardware, these safety standards consist of the guidelines and procedures published in MASH (*5*). According to TL-4 of MASH, longitudinal barrier systems must be subjected to three full-scale vehicle crash tests:

1) Test Designation 4-10 with a 2,425-lb small car (designated 1100C) impacting at a speed of 62 mph and angle of 25 degrees.
2) Test Designation 4-11 with a 5,000-lb pickup truck (designated 2270P) impacting at a speed of 62 mph and angle of 25 degrees.
3) Test Designation 4-12 with a 22,000-lb single-unit truck (designated 10000S) impacting at 56 mph and 15 degrees.

Evaluation criteria for full-scale vehicle crash testing are based on three appraisal areas: (1) structural adequacy; (2) occupant risk; and (3) vehicle trajectory after collision. These evaluation criteria are defined in greater detail in MASH. The full-scale vehicle crash tests were conducted and reported in accordance with the procedures provided in MASH.

FULL-SCALE CRASH TEST SFH-1 (MASH TEST DESIGNATION 4-11)

The 5,021-lb Dodge Ram pickup truck impacted the barrier at a speed of 63.9 mph and an angle of 24.7 degrees. Sequential photographs and system and vehicle damage are shown in FIGURE 3. Initial vehicle impact was to occur $51^{3}/_{16}$ in. upstream from the joint between barriers 5 and 6, which was selected based on recommendations for rigid barrier tests in MASH and verified though LS-DYNA simulation (*4*).

Upon impact, barriers 5 and 6 began to deflect backward. At 0.160 seconds, the maximum lateral dynamic deflection was 11.2 in. at the upstream end of concrete barrier 6. At 0.206 seconds, the vehicle was parallel to the system, and at 0.540 seconds, the vehicle exited the system.

Barrier damage consisted of contact marks, concrete spalling and gouges, and hairline concrete cracks. The length of vehicle contact along the barrier was approximately 15 ft – ¼ in. The front faces of barriers 5 and 6 were gouged from wheel contact. The joints between barriers 5 and 6 maintained strength during and after impact, but upon removal of the joints, several concrete pieces between the splice bolts on the frontside of the beams had fractured off up to the reinforcement. The first two posts downstream from the splice between barriers 5 and 6 had contact marks along the front face and part of the upstream face. Permanent set was approximately ⅞ in. The working width of the system was found to be 33.5 in.

The majority of the vehicle damage was concentrated on the left-front corner and left side of the vehicle where the impact occurred. The left-front control arm disengaged, and the left-front tire deflated and released from the rim. The entire left side of the vehicle had scrapes and dents. The maximum occupant compartment deformation was 1 in. located at the left-side driver's door below seat level, and all occupant compartment deformations were below the limits established in MASH.

The calculated occupant impact velocities (OIVs) and maximum 0.010-sec occupant ridedown accelerations (ORAs) in both the longitudinal and lateral directions were within the suggested limits provided in MASH. Therefore, test SFH-1 conducted on the energy-absorbing

barrier was determined to be acceptable according to MASH safety performance criteria for test designation 4-11. More comprehensive tests results are presented in Schmidt, et al. (*14*).

To determine if lateral accelerations and barrier forces were reduced, MASH crash tests with 2270P vehicles with a vertical-faced concrete barrier were desired for comparison. However, crash test data for rigid vertical barriers were not available, so two other MASH crash tests were utilized: test 420020-3 with a 2270P pickup truck impacting a single-slope barrier attached to a bridge deck (*15*) and test KSFRP-1 with a 2270P pickup truck impacting a vertical precast concrete barrier attached to a fiber-reinforced polymer (FRP) deck (*16*). The longitudinal and lateral vehicle accelerations from each test, as measured at the vehicle's center of gravity, were processed using a 50-msec moving average. The 50-msec moving average vehicle accelerations were then combined with the uncoupled yaw angle versus time data in order to estimate the vehicular loading applied to the barrier system.

The test comparison matrix and the force comparison plots for the 2270P vehicle are shown in FIGURE 4. The peak lateral barrier forces were reduced 38 percent and 23 percent in the energy-absorbing barrier compared to tests 420020-3 and KSFRP-1, respectively. The MASH-recommended CFC 180 10-ms average peak lateral acceleration was reduced 47 percent and 25 percent in the energy-absorbing barrier compared to tests 420020-3 and KSFRP-1, respectively. When compared to test 420020-3, the lateral OIV was reduced 29 percent and the longitudinal OIV was reduced 27 percent. Lateral and longitudinal ORA did not change significantly.

0.000 sec

0.100 sec

0.200 sec

0.300 sec

0.400 sec

0.500 sec

(a) Sequential Photos

(b) System Damage

(c) Joint at Barriers 5 and 6

(d) Post Contact

(e) Vehicle Damage

FIGURE 3 System and vehicle damage in test SFH-1, (a) sequential photos, (b) system damage, (c) joint at barriers 5 and 6, (d) post contact, and (e) vehicle damage.

Description	Concrete Single Slope Barrier	Vertical Precast Concrete on FRP Deck	Energy-Absorbing Barrier (Primary Accelerometer)	Energy-Absorbing Barrier (Secondary Accelerometer)
Test No.	420020-3	KSFRP-1	SFH-1	SFH-1
Reference	(*15*)	(*16*)	(*14*)	(*14*)
Vehicle	2270P	2270P	2270P	2270P
Test Inertial Weight (lb)	5036	5009	5021	5021
Impact Velocity (mph)	63.8	61.1	63.4	63.4
Impact Angle (degrees)	24.8	25.9	24.8	24.8
Impact Severity (kip-ft)	120.6	119.3	118.5	118.5
Lateral OIV (ft/s)	29.9	25.3	21.3	21.2
Longitudinal OIV (ft/s)	22.0	17.7	17.6	16.0
Lateral ORA (g's)	11.7	6.3	8.4	10.1
Longitudinal ORA (g's)	5.3	6.5	4.8	9.6
CFC 180 10-ms Average Peak Lateral Acceleration (g's)	28.1	19.7	14.8	15.8
Peak Perpendicular Barrier Force (kips)	93	75	58	62

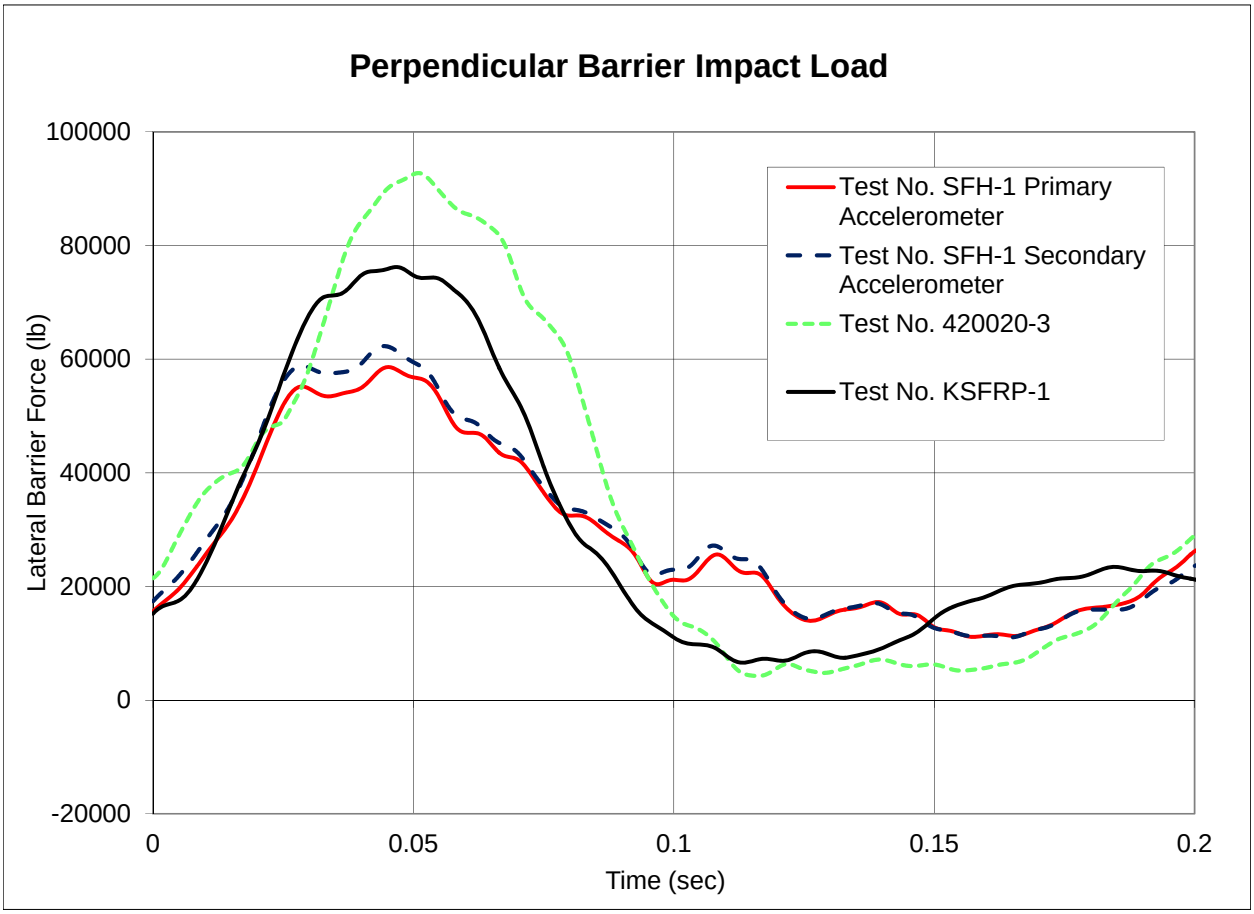

FIGURE 4 Force comparison of 2270P vehicle impacts.

FULL-SCALE CRASH TEST SFH-2 (MASH TEST DESIGNATION 4-10)

The 2,406-lb Kia Rio small car impacted the barrier at a speed of 64.3 mph and an angle of 24.7 degrees. Sequential photographs and vehicle and system damage are shown in FIGURE 5. Initial vehicle impact was to occur $18^{5}/_{16}$ in. upstream of the joint between barriers 7 and 8, which was selected based on the recommendation for rigid barrier tests in MASH and verified through LS-DYNA simulation. The impact point was downstream from test SFH-1 so damage could be distinguished between the two tests.

Upon impact, barriers 7 and 8 began to deflect backward. At 0.142 seconds, the maximum lateral dynamic barrier deflection was 7.1 in. at the top downstream end of barrier 7. At 0.250 seconds, the vehicle was parallel to the system, and at 0.330 seconds, the vehicle exited the system.

Barrier damage consisted of gouging and contact marks on the front face of concrete beams 7 and 8 and cuts in the elastomer posts. The length of the vehicle contact along the barrier was approximately 12 ft – 7 in. The first post downstream from the joint between barriers 7 and 8 had a 3½-in. wide x 7-in. tall contact mark on the upstream face and was cut along the length of the front face 3 in. above the groundline that had a maximum depth of ½ in. due to contact with the vehicle's rim. The second post downstream from the joint between barriers 7 and 8 was cut along the length of the front face located 4 in. above the groundline that had a maximum depth of 2 in. The upstream corner of the front face had contact marks 5¼ in. wide x 7 in. tall. The vehicle re-contacted the system after exiting the system initially.

The permanent set of the barrier was approximately 1¾ in., which was measured at the joint between barriers 7 and 8. The working width of the system was found to be 28.8 in.

The majority of the vehicle damage was concentrated on the left-front corner and left side of the vehicle where the impact occurred. The front windshield was cracked. The hood and left fender were torn and crushed inward. A 6¾-in. long cut was found in the left-front door. The left-front tire was deflated, with gouges around the outer rim. The A-pillar was dented, and the left-front window shattered from contact with the dummy's head.

The maximum occupant compartment deformation was 3¼ in. in the left side-door, which was within the deformation limits established in MASH. The maximum OIVs and ORAs in both the longitudinal and lateral directions were within the suggested limits provided in MASH. Therefore, test SFH-2 conducted on the energy-absorbing barrier was determined to be acceptable according to MASH safety performance criteria for test designation 4-10. More comprehensive tests results are presented in Schmidt, et al. (*14*).

Similar to the 2270P crash test comparisons, MASH crash tests with 1100C vehicles with a vertical-faced concrete barrier were desired for comparison. However, crash test data for rigid vertical concrete barriers were not available, so two other MASH crash tests were utilized: test 420020-6 with an 1100C small car impacting a vertical steel median gate (*17*) and test 2214NJ-1 with an 1100C small car impacting a New Jersey concrete barrier (*18*). The vehicular loading applied to the barrier system was calculated for each test.

The test comparison matrix and the force comparison plots for the 1100C vehicle are shown in FIGURE 6. The lateral peak barrier forces were reduced 15 percent and 16 percent when compared to tests 420020-6 and 2214NJ-1, respectively. The MASH-recommended CFC 180 10-ms average peak lateral acceleration increased 23 percent when compared to test 420020-6 and decreased 21 percent when compared to test 2214NJ-1. The peak lateral acceleration may have been lower in the steel median gate; since, it had lower inertia, may have deformed more, and may have distributed load more efficiently than concrete. Additionally, the energy-absorbing

barrier reduced lateral OIV value 31 percent as compared to test 2214NJ-1. Lateral OIV and lateral and longitudinal ORA values were similar to the other tests.

0.000 sec

0.100 sec

0.200 sec

0.300 sec

0.400 sec

0.500 sec

(a) Sequential Photos

(b) System Damage

(c) System Damage

(d) Post Damage

(e) Vehicle Damage

FIGURE 5 System and vehicle damage in test SFH-2, (a) sequential photos, (b) system damage, (c) system damage, (d) post damage, and (e) vehicle damage.

Description	Vertical Steel Median Gate	New Jersey Concrete Barrier	Energy-Absorbing Barrier (Primary Accelerometer)	Energy-Absorbing Barrier (Secondary Accelerometer)
Test No.	420020-6	2214NJ-1	SFH-2	SFH-2
Reference	(*17*)	(*18*)	(*14*)	(*14*)
Vehicle	1100C	1100C	1100C	1100C
Test Inertial Weight (lb)	2424	2414	2406	2406
Impact Velocity (mph)	62.6	60.8	64.3	64.3
Impact Angle (degrees)	24.6	26.1	24.8	24.8
Impact Severity (kip-ft)	55.0	57.8	58.5	58.5
Lateral OIV (ft/s)	31.2	35.1	25.6	24.3
Longitudinal OIV (ft/s)	26.6	16.1	26.6	26.2
Lateral ORA (g's)	6.4	8.1	8.2	7.4
Longitudinal ORA (g's)	4.0	5.5	5.1	4.9
CFC 180 10-ms Average Peak Lateral Acceleration (g's)	26.5	37.0	32.5	29.3
Peak Perpendicular Barrier Force (kips)	54.8	55.2	48.4	46.4

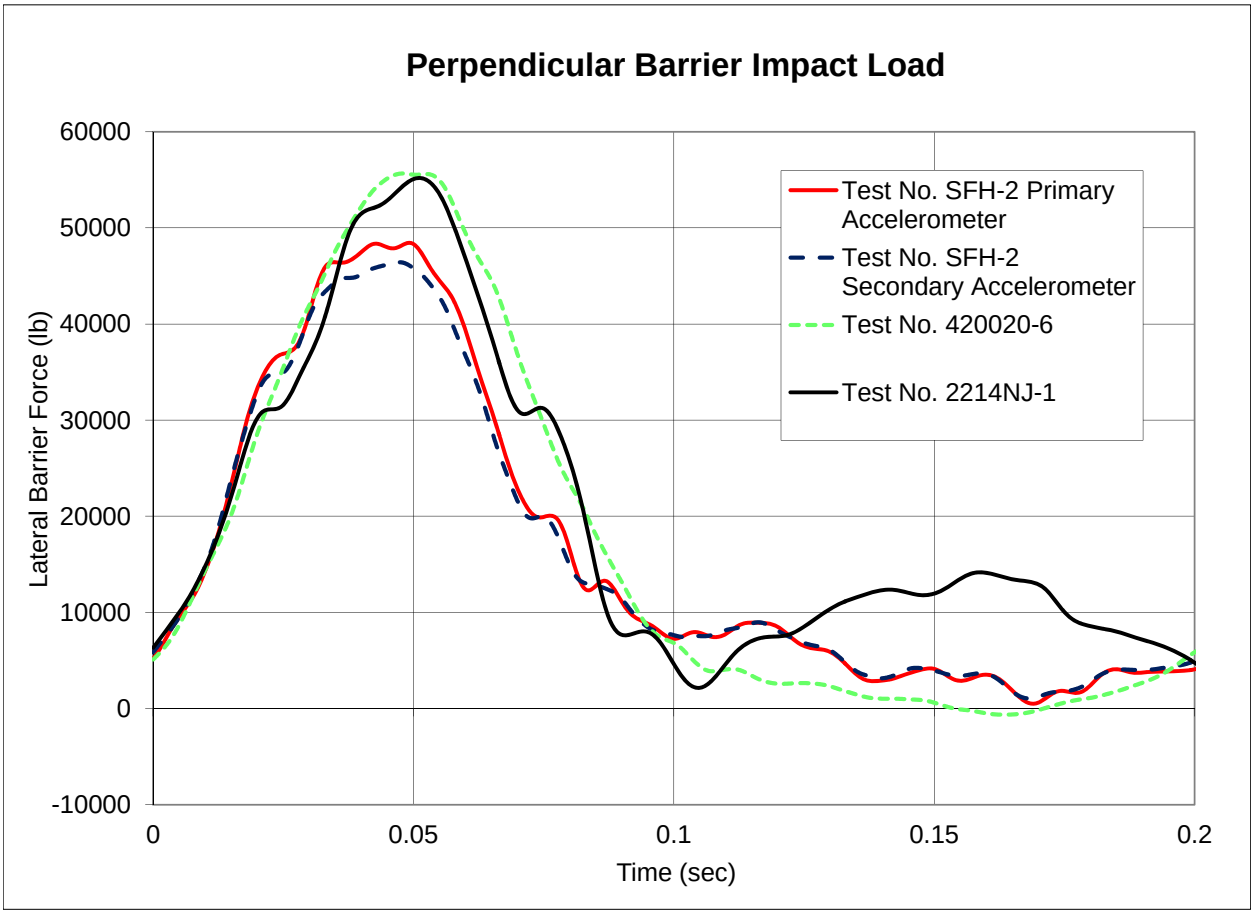

FIGURE 6 Test Comparison of 1100C vehicle impacts.

FULL-SCALE CRASH TEST SFH-3 (MASH TEST DESIGNATION 4-12)

The installation for test SFH-3 was similar to the system used in tests SFH-1 and SFH-2. Previously damaged components were moved out of the impact region. The 21,746-lb single-unit truck impacted the barrier at a speed of 56.5 mph and an angle of 14.8 degrees. Sequential photographs and vehicle and system damage are shown in FIGURE 7.

Initial vehicle impact was to occur 60 in. upstream from the joint between barriers 5 and 6, which was selected based on recommendation for rigid barrier tests in MASH and verified through LS-DYNA simulation. Upon impact, barriers 5 and 6 began to deflect backward. At 0.388 seconds, the maximum lateral dynamic barrier deflection at the top of the upper tube at the upstream end of barrier 6, was 15.1 in. At 0.394 seconds, the maximum lateral dynamic barrier deflection at the top upstream end of concrete barrier 6 and was 13.9 in. At 0.326 seconds, the vehicle was parallel to the system. At 0.989 seconds, the cargo box reached a maximum roll angle of 39.1 degrees, and at 1.320 seconds, the vehicle exited the system.

Barrier damage consisted of contact marks and gouging on the front face of the concrete beams, cracking and spalling at the joint connections, contact marks along the top of the concrete beams and along the upper tube assembly, and contact marks on the elastomer posts. The length of the vehicle contact along the barrier was approximately 59 ft – 3 in. The front faces and bottom edges of barriers 5 and 6 were gouged from wheel contact with the system. The first post upstream from the joint between barriers 5 and 6 had a ¼-in. deep x 1-in. diameter semicircular cut on the front face from contact with the left-front tire lug nuts. The top of barriers 6, 7, and 8 were gouged from contact with the underside of the cargo box. The joints between barriers 4 and 5 through barriers 8 and 9 maintained strength during and after impact, but upon removal of the joints, several concrete pieces on the lower half of the beams had fractured off up to the reinforcement. The permanent set of the barrier was approximately 1½ in., which was measured in the field at the upstream end of barrier 6. The working width of the system was found to be 60.2 in. due to the cargo box extension behind the rail.

The majority of the vehicle damage was concentrated on the left-front corner of the vehicle where the impact occurred and the frame under the cargo box. The front U-bolts and centering pin were fractured, and the front axle displaced rearward. The left fender had multiple cracks and gouges. The cargo box had multiple dents and scrapes as well as a 3-in. long tear. The left-front and left-rear tires were deflated. All of the additional U-bolts and shear plates that were added to strengthen the box-frame connection were bent. The maximum occupant compartment deformations was 2⅜ in. in the wheel well and toepan area. Therefore, test SFH-3 conducted on the energy-absorbing barrier was determined to be acceptable according to MASH safety performance criteria for test designation 4-12. More comprehensive tests results are presented in Schmidt, et al. (14).

While it was not a design criteria to reduce lateral accelerations for the single-unit truck, MASH test designation 4-12 crash tests with rigid concrete barriers were desired to compare barrier forces. However, test data was not available to compare barrier forces. The vehicular loading applied to the barrier system in test SFH-3 was calculated the same as previously. From the data analysis, the perpendicular impact force was determined, as shown in FIGURE 8. The maximum perpendicular, or lateral, load imparted to the barrier was 105 kips and 95 kips, as determined by the primary and secondary accelerometers, respectively.


0.000 sec


0.200 sec


0.400 sec


0.600 sec


0.800 sec


1.000 sec

(a) Sequential Photos

(b) System Damage

(c) System Damage


(d) Barriers 6 and 7 Damage

(e) Vehicle Damage

FIGURE 7 System and vehicle damage in test SFH-3, (a) sequential photos, (b) system damage, (c) system damage, (d) barriers 6 and 7 damage, and (e) vehicle damage.

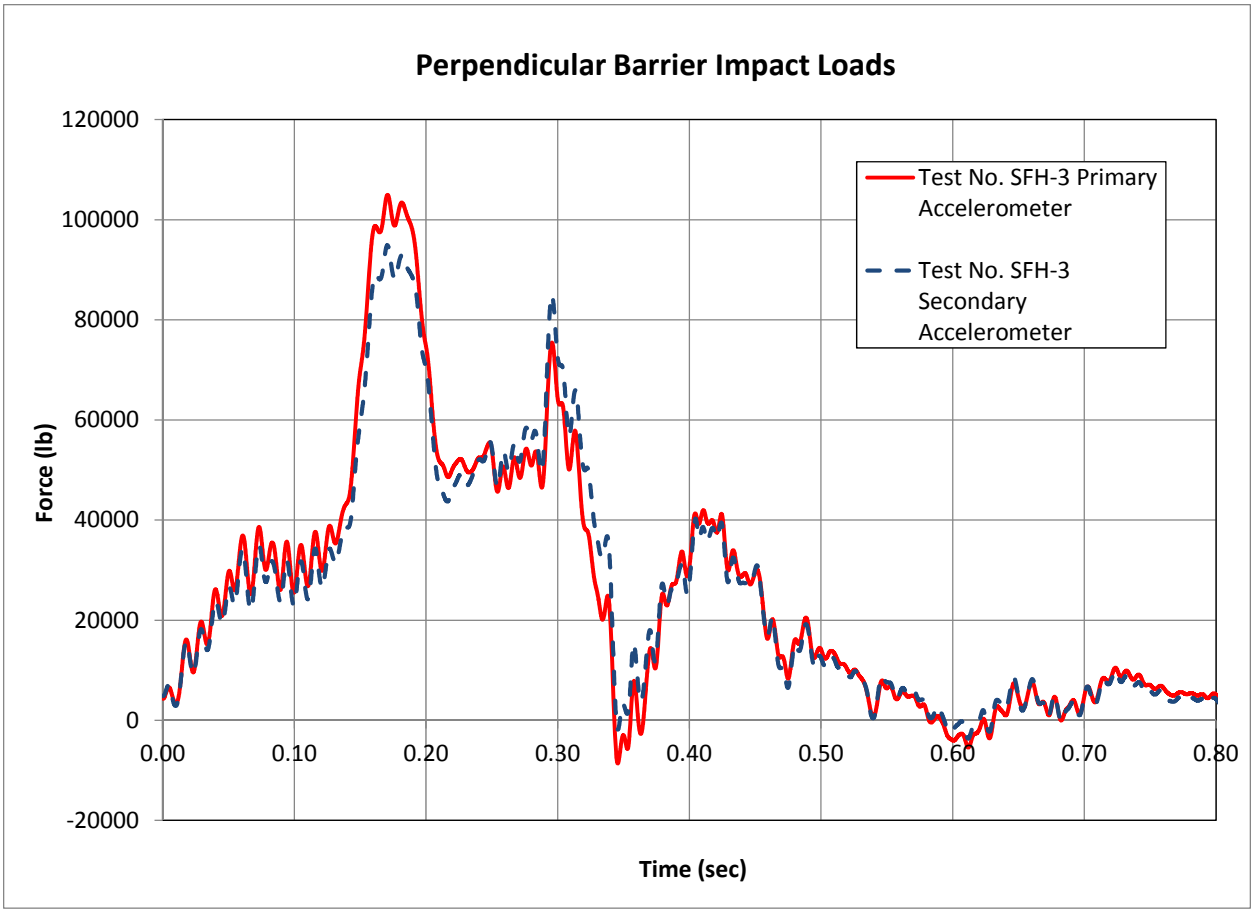

FIGURE 8 Perpendicular barrier forces in test SFH-3.

CONCLUSIONS AND RECOMMENDATIONS

A restorable and reusable energy-absorbing roadside/median barrier was designed and evaluated according to MASH TL-4 safety performance criteria (*1-4,14*). The new barrier was configured to fit in current roadside and median footprints and reduce lateral accelerations and forces to passenger vehicle occupants.

Three full-scale crash tests were conducted and met all MASH TL-4 safety performance requirements. A 30 percent reduction in lateral acceleration was desired for passenger vehicle impacts as compared to similar impacts with rigid concrete barriers. While rigid barriers provide occupant risk measures below the maximum limits defined in MASH, the occupant risk values are often over the preferred limits, especially for small car impacts. The occupant safety measures showed reductions from rigid barrier crash tests and were below preferred limits in all of the full-scale crash tests conducted.

In test SFH-1, the peak lateral acceleration was reduced 47 percent as compared to an impact with a concrete single-slope barrier. The lateral and longitudinal OIV values were also reduced 29 and 27 percent, respectively. In test SFH-2, the peak lateral acceleration was reduced 21 percent and the lateral OIV was reduced 31 percent as compared to an impact with a concrete New Jersey-shaped barrier. The barrier forces were also reduced 38 percent and 16 percent in tests SFH-1 and SFH-2, respectively. Therefore, the barrier provided significant reductions in occupant risk measures for passenger vehicle impacts, with over a 30 percent reduction for pickup truck impacts and a slightly less reduction for small car impacts.

The barrier also adequately contained and redirected the MASH TL-4 single-unit truck. The structural capacity was sufficient to sustain the maximum perpendicular load of 105 kips with only minimal damage to the system.

The barrier restored to within 1¾ in. of its original placement in all three crash tests, and the permanent set was isolated to the joint nearest the impact point in each of the tests. The permanent set should not affect the performance of repeated impacts on the system and is considered negligible. The permanent set of the barrier was likely enhanced by the joint and post damage observed during the tests, and may be minimized if further damage can be mitigated.

Minimal damage occurred in all of the crash tests but should not prohibit the system from being reusable. The same system components were reused for the three crash tests. Enhancements are recommended to further optimize system behavior and minimize system damage including:

- Strengthening the concrete beams near the ends to minimize spalling and cracking at the joints.
- Changing the concrete mix, increasing the concrete density, or adding reinforcing fibers to the concrete to minimize surface gouging and increase strength. It is unlikely that concrete gouges can be completely eliminated, as this is common in all concrete barriers.
- Reducing the clear opening below the concrete beam, widening the concrete beams, or modifying the posts to minimize wheel contact with the posts.

Further research is recommended to transition and terminate the longitudinal barrier. The barrier system was tested with no upstream or downstream anchorages to evaluate the maximum deflection and backward rotation that could be experienced by the barrier, similar to a long installation when the termination is far from the impact region. However, the upstream and downstream ends of the barrier should be transitioned into another barrier system, such as a rigid concrete barrier. The rigid concrete barrier could then be protected with a crash cushion or be extended as a rigid longitudinal barrier. The effects of stiffness transitions and end constraints at the ends of the barrier will be evaluated in future phases of this research effort. In addition, other applications for the energy-absorbing barrier, such as bridge rails, may be explored.

ACKNOWLEDGMENTS

The authors wish to acknowledge several sources that made a contribution to this project: (1) the Federal Highway Administration and the Nebraska Department of Roads for sponsoring this project and (2) MwRSF personnel for constructing the system and conducting the crash tests.

REFERENCES

1. Schmidt, J.D., R.K. Faller, D.L. Sicking, J.D. Reid, K.A. Lechtenberg, R.W. Bielenberg, S.K. Rosenbaugh, and J.C. Holloway. *Development of a New Energy-Absorbing Roadside/Median Barrier System with Restorable Elastomer Cartridges*. MwRSF Research Report No. TRP-03-281-13. Midwest Roadside Safety Facility, University of Nebraska-Lincoln, 2013.

2. Schmidt, J.D. *Development of a New Energy-Absorbing Roadside/Median Barrier System with Restorable Elastomer Cartridges*. A dissertation, University of Nebraska-Lincoln, 2012.

3. Schmidt, J.D., T.L. Schmidt, R.K. Faller, D.L. Sicking, J.D. Reid, K.A. Lechtenberg, R.W. Bielenberg, S.K. Rosenbaugh, and J.C. Holloway. *Evaluation of Energy Absorbers for Use in a Roadside/Median Barrier*. MwRSF Research Report No. TRP-03-280-14. Midwest Roadside Safety Facility, University of Nebraska-Lincoln, 2014.

4. Schmidt, J.D., S.K. Rosenbaugh, R.K. Faller, R.W. Bielenberg, J.D. Reid, J.C. Holloway, K.A. Lechtenberg, and J.E. Kohtz. *Design and Evaluation of an Energy-Absorbing, Reusable, Roadside/Median Barrier.* MwRSF Research Report No. TRP-03-317-15. Midwest Roadside Safety Facility, University of Nebraska-Lincoln, 2015.

5. AASHTO. *Manual for Assessing Safety Hardware (MASH)*. Washington, D.C., 2009.

6. Reid, J.D., R.K. Faller, and D.L. Sicking. High-Speed Crash Barrier Investigation Using Simulation. Crashworthiness, Occupant Protection, and Biomechanics in Transportation Systems, Applied Mechanics Division (AMD) – Vol. 246, BED – Vol. 49, 2000 ASME International Mechanical Engineering Congress and Exposition, Orlando, Florida, 2000.

7. Reid, J.D., R.K. Faller, J.C. Holloway, J.R. Rohde, and D.L. Sicking. A New Energy-Absorbing High-Speed Safety Barrier. *Transportation Research Record: Journal of the Transportation Research Board, No. 1851*, Transportation Research Board of the National Academies, Washington, D.C., January 2003, pp. 53-64.

8. Bielenberg, R.W. and J.D. Reid. Modeling of Crushable Foam for the SAFER Racetrack Barrier. *8th International LS-DYNA Users Conference,* Simulation 2004, Dearborn, Michigan, 2004.

9. Melvin, J.W., P.C. Begeman, R.K. Faller, D.L. Sicking, S.B. McClellan, E. Maynard, M.W. Donegan, A.M. Mallott, and T.W. Gideon. Crash Protection of Stock Car Racing Drivers – Application of Biomedical Analysis of Indy Car Crash Research. *Stapp Car Crash Journal No. 50*, The Stapp Association, 50th Stapp Car Crash Conference, Dearborn, Michigan, pp. 415-428, 2006.

10. Faller, R.K., R.W. Bielenberg, D.L. Sicking, J.R. Rohde, and J.D. Reid. Development and Testing of the SAFER Barrier – Version 2, SAFER Barrier Gate, and Alternative Backup Structure. *Proceedings of the 2006 SAE Motorsports Engineering Conference and Exhibition,* Paper No. 2006-01-3612, Publication No. P-399, Dearborn, Michigan, 2006.

11. Faller, R.K., D.L Sicking, J.R. Rohde, J.D. Reid, E.A. Keller, R.W. Bielenberg, J.C. Holloway, K.H. Addink, and K.A. Polivka. *High-Impact, Energy-Absorbing Vehicle Barrier System*. U.S. Patent No. 6,926,461 B1, August 9, 2005.

12. Faller, R.K., J.R. Rohde, D.L. Sicking, R.W. Bielenberg, J.D. Reid, J.C. Holloway, and K.A. Polivka. *High-Impact, Energy-Absorbing Vehicle Barrier System.* U.S. Patent No. 7,410,320 B2, August 12, 2008.

13. Bligh, R.P., N.M. Sheikh, A.Y. Obu-Odeh, and W.L. Menges. *Evaluation of Barriers for Very High Speed Roadways*. Report No. FHWA/TX-10/0-6071-2, Texas A&M Transportation Institute, Texas A&M University, 2010.

14. Schmidt, J.D., T.L. Schmidt, S.K. Rosenbaugh, R.K. Faller, R.W. Bielenberg, J.D. Reid, J.C. Holloway, and K.A. Lechtenberg. *MASH TL-4 Testing and Evaluation of the RESTORE Barrier*. MwRSF Research Report No. TRP-03-318-15. Midwest Roadside Safety Facility, University of Nebraska-Lincoln, 2015.

15. Williams, W.F., R.P. Bligh, and W.L. Menges, *MASH Test 4-11 of the TxDOT Single Slope Bridge Rail (Type SSTR) on Pan-Formed Bridge Deck.* Report No. FHWA/TX-11/9-1002-3. Texas A&M Transportation Institute, Texas A&M University, 2011.

16. Schmidt, J.D., R.K. Faller, K.A. Lechtenberg, D.L. Sicking, and J.D. Reid. *Development and Testing of a New Vertical-Faced Temporary Concrete Barrier for use on Composite Panel Bridge Decks.* MwRSF Research Report No. TRP-03-220-09. Midwest Roadside Safety Facility, University of Nebraska-Lincoln, 2009.

17. Bligh, R.P., D.R. Arrington, N.M Sheikh, C. Silvestri, and W.L. Menges. *TL-4 Median Barrier Gate.* Report No. FHWA/TX-11/9-1002-2. Texas A&M Transportation Institute, Texas A&M University, 2011.

18. Polivka, K.A., R.K. Faller, D.L. Sicking, J.R. Rohde, B.W. Bielenberg, J.D. Reid, and B.A. Coon. *Performance Evaluation of the Permanent New Jersey Safety Shape Barrier – Update to NCHRP 350 Test No. 4-10 (2214NJ-1).* MwRSF Research Report No. TRP-03-177-06. Midwest Roadside Safety Facility, University of Nebraska-Lincoln, 2006.